Escherichia coli responds to environmental changes using enolasic degradosomes and stabilized DicF sRNA to alter cellular morphology

Oleg N. Murashko[a] and Sue Lin-Chao[a,1]

[a]Institute of Molecular Biology, Academia Sinica, Taipei 11529, Taiwan

Edited by Joe Lutkenhaus, University of Kansas Medical Center, Kansas City, KS, and approved August 11, 2017 (received for review March 9, 2017)

Escherichia coli **RNase E is an essential enzyme that forms multicomponent ribonucleolytic complexes known as "RNA degradosomes." These complexes consist of four major components: RNase E, PNPase, RhlB RNA helicase, and enolase. However, the role of enolase in the RNase E/degradosome is not understood. Here, we report that presence of enolase in the RNase E/degradosome under anaerobic conditions regulates cell morphology, resulting in *E. coli* MG1655 cell filamentation. Under anaerobic conditions, enolase bound to the RNase E/degradosome stabilizes the small RNA (sRNA) DicF, i.e., the inhibitor of the cell division gene *ftsZ*, through chaperon protein Hfq-dependent regulation. RNase E/enolase distribution changes from membrane-associated patterns under aerobic to diffuse patterns under anaerobic conditions. When the enolase-RNase E/degradosome interaction is disrupted, the anaerobically induced characteristics disappear. We provide a mechanism by which *E. coli* uses enolase-bound degradosomes to switch from rod-shaped to filamentous form in response to anaerobiosis by regulating RNase E subcellular distribution, RNase E enzymatic activity, and the stability of the sRNA DicF required for the filamentous transition. In contrast to *E. coli* nonpathogenic strains, pathogenic *E. coli* strains predominantly have multiple copies of sRNA DicF in their genomes, with cell filamentation previously being linked to bacterial pathogenesis. Our data suggest a mechanism for bacterial cell filamentation during infection under anaerobic conditions.**

RNase E | RNA decay | protein subcellular distribution | anaerobic conditions | cell shape

Posttranscriptional regulation of RNAs is an important molecular mechanism for controlling gene expression, requiring various ribonucleases (RNases), including RNase E, which is an essential single-stranded endo-RNase involved in RNA processing and decay (1). RNase E has N-terminal catalytic and C-terminal scaffolding domains (2), with the latter responsible for assembling multicomponent ribonucleolytic complexes termed "RNA degradosomes." Degradosomes consist of RNase E, PNPase 3′→5′ exoribonuclease, RhlB RNA helicase, and the glycolytic enzyme enolase (3, 4). Therefore, they can act on RNA internally (by RNase E) and/or externally (by PNPase) to catalyze the degradation of RNA into short fragments. Immunogold electron microscopy has shown that degradosomes exist in vivo and are tethered to the cytoplasmic membrane through the N-terminal region of RNase E (5). Binding of the N-terminal catalytic domain (amino acids 1–499) to the membrane stabilizes protein structure and increases both RNA cleavage activity and substrate affinity (6). Global analyses of aerobic *Escherichia coli* RNA degradosome functioning using DNA microarrays showed that decay of some mRNAs in vivo depends on the action of assembled degradosomes, whereas other mRNAs are impacted by degradosome proteins functioning independently of the complex (7–9). Some minor components of the degradosome, such as the inhibitors of RNase E, RraA and RraB (10), and ribosomal protein L4 (11), affect the stability of subsets of transcripts. Structural features or biochemical factors that target specific classes of mRNAs for degradosomal decay may exist.

E. coli is a metabolically versatile bacterium that is able to grow under aerobic and anaerobic conditions. Adaptation to environments with different O_2 concentrations, which is vital for *E. coli* competitiveness and growth, requires reprogramming of gene expression and cell metabolism. *E. coli* uses one of three metabolic modes to support growth (12, 13), which depend on the availabilities of electron donors and acceptors. In the presence of O_2, aerobic respiration allows complete oxidation of a growth substrate (such as glucose) and therefore is the most productive mode. Two alternative metabolic modes are available in the absence of O_2, one of which is anaerobic respiration, which yields less energy than aerobic respiration because the substrate is only partially oxidized. The other O_2-deficient mode is fermentation, which is the least productive mode since energy is generated only by substrate level phosphorylation. Thus, changes in *E. coli* physiology are provoked by changes in O_2 availability.

The discovery of the multicomponent ribonucleolytic complexes associated with *E. coli* RNase E and their extensive characterization in vivo and in vitro have yielded a wealth of information regarding the structure and function of the complexes under aerobic growth conditions (see ref. 14 for a review). Enolase is a key enzyme of glycolysis, a process that generates ATP by converting glucose to pyruvate in either the presence (aerobic) or absence (anaerobic) of oxygen. Anaerobic glycolysis is thought to have been the primary means of energy production in ancient organisms before oxygen was at high atmospheric concentrations. This metabolic pathway is particularly essential under the anaerobic conditions faced by *E. coli* and other pathogenic bacteria in the intestine. In this paper we address the specific function of enolase in the bacterial degradosome under anaerobic growth (sometimes also referred to as "oxygen-limited growth") conditions.

Significance

The prevalent habitat of *Escherichia coli* is the predominantly anaerobic environment of the gastrointestinal tract of humans and other warm-blooded organisms. We found that, under anaerobic conditions, the presence of enolase in the RNA degradation machinery regulates cell morphology and induces *E. coli* filamentation by stabilizing a small RNA, DicF, that inhibits the cell division gene *ftsZ*. Cell filamentation has previously been linked to bacterial pathogenesis. In contrast to *E. coli* nonpathogenic strains, pathogenic *E. coli* strains possess multiple copies of sRNA DicF in their genomes. Our data provide a mechanism by which bacterial cells can adopt a filamentous form during infection under anaerobic conditions.

Author contributions: O.N.M. and S.L.-C. designed research; O.N.M. performed research; S.L.-C. contributed new reagents/analytic tools; O.N.M. and S.L.-C. analyzed data; O.N.M. and S.L.-C. wrote the paper; and S.L.-C. was the Principal Investigator.

The authors declare no conflict of interest.

This article is a PNAS Direct Submission.

Freely available online through the PNAS open access option.

[1]To whom correspondence should be addressed. Email: mbsue@gate.sinica.edu.tw.

This article contains supporting information online at www.pnas.org/lookup/suppl/doi:10.1073/pnas.1703731114/-/DCSupplemental.

We found that under anaerobic conditions *E. coli* MG1655 cells are characterized by a predominantly (~70%) filamentous morphology (>5 μm in length). Our study shows that in response to oxygen-limited conditions concentrations of RNase E protein are decreased, and its subcellular distribution is altered. We demonstrate that the anaerobically induced filamentous morphology is the result of a specific function of the enolase-bound RNA degradosome through small RNA DicF stabilization and FtsZ protein expression. Our results demonstrate the unique role of enolase for RNase E/degradosome-based regulation of bacterial morphology in response to oxygen-limited conditions and may provide a mechanistic explanation for some virulent *E. coli* strains whose morphological differentiation from rod to filamentous shape occurs under significantly low oxygen tension.

Results

RNase E Regulates Cell Filamentous Morphology and Is Oxygen-Level Dependent. We determined RNase E protein levels in *E. coli* MG1655 under aerobic and anaerobic conditions by Western blotting and found that RNase E protein levels were significantly (~4.0-fold) lower under anaerobic conditions (Fig. 1*A* and Fig. S1*A*). The decreased level of RNase E is due to active degradation of the protein (Fig. S1*B*). Microscopic observations showed that under anaerobic conditions *E. coli* MG1655 cells are characterized by a filamentous morphology (Fig. 1*B*), with ~70% of the cells being >5 μm in length (Fig. 1*C*, *Upper*). In comparison, ~99.5% of cells of the same strain grown under aerobic conditions are <5 μm long (Fig. 1*C*, *Lower*). The cells that are filamenting show OD increases for a long time, but the increase was slower than in cells grown under aerobic conditions (Fig. S2*A*).

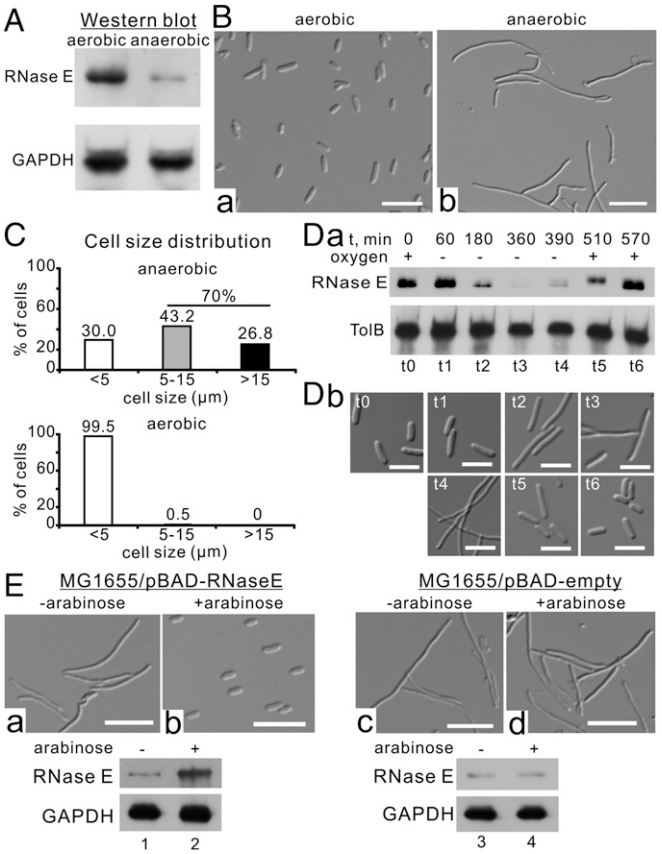

Fig. 1. RNase E is a key regulator of cell filamentation under anaerobic conditions. (*A*) Endogenous expression levels of RNase E under aerobic and anaerobic conditions. Whole-cell extracts were analyzed by SDS/PAGE and immunoblotted with the indicated antibodies. (*B*) *E. coli* MG1655 cell morphology under aerobic (*B*, *a*) and anaerobic (*B*, *b*) conditions. (Scale bars, 5 μm.) (*C*) Cell-size distribution of *E. coli* MG1655 cells under aerobic and anaerobic conditions. The lengths of cells were measured using the image analysis package MetaMorph (*SI Materials and Methods*). (*D*) RNase E protein levels (*D*, *a*) and cell morphology (*D*, *b*) under aerobic–anaerobic–aerobic alternating growth conditions. (Scale bars, 5 μm.) (*E*) Arabinose-induced expression of RNase E under anaerobic conditions. (*Upper*) Cell morphology. (Scale bars, 5 μm.) (*Lower*) RNase E protein levels.

Using aerobic–anaerobic–aerobic alternating growth conditions (Fig. S1*D*), we found that protein levels of chromosomal (untagged) or ectopically expressed RNase E using an arabinose-inducible promoter from the pBAD plasmid (Flag-tagged) decreased after shifting to anaerobic conditions but then were restored after reverting to aerobic conditions (Fig. 1 *D*, *a*, lanes t1–t6 and Fig. S1*C*, respectively), indicating that the amount of RNase E is correlated to the amount of oxygen. This additional experiment indicates that decreased RNase E protein levels are mainly due to active degradation of the protein. Cell morphology also cycled through rod–filamentous–rod shapes in accordance with aerobic–anaerobic–aerobic conditions (Fig. 1 *D*, *b*). Cell filamentation was completely resolved within ~3 h after shifting back to aerobic conditions or on RNase E overexpression (Fig. 1 *E*, *a* and *b* and Movie S1). In contrast, cells transformed with the empty pBAD vector maintained a filamentous morphology under the same culture conditions (Fig. 1 *E*, *c* and *d*). Thus, our data demonstrate that acquisition of a filamentous morphology under anaerobic conditions is correlated with reduced RNase E protein levels.

Cell Filamentation Under Anaerobic Conditions Requires Enolase-Bound RNA Degradosomes. Since RNase E exists as multienzyme complexes (the RNA degradosomes) in cells (5), we investigated the possibility that RNA degradosomes are involved in *E. coli* acquiring the filamentous morphology under anaerobic conditions. We used the *E. coli* MG1655 strain to construct defined isogenic mutant strains (Fig. S3). We generated a MG1655 derivative that lacked degradosome formation by deleting amino acid residues 500–1,061 of the scaffolding domain of RNase E (hereafter Rned500–1061; see *SI Materials and Methods*). Rned500–1061 possesses only the N-terminal 499-aa residues of RNase E (Fig. 2 *A*, *c* and *d*). As shown in Fig. 2, under anaerobic conditions, Rned500–1061 had uniformly rod-shaped cells (~2.0–2.5 μm) (Fig. 2 *A*, *c* and *d*), in contrast to MG1655 (Fig. 2 *A*, *a* and *b*), suggesting involvement of degradosome components in cell filamentation under anaerobic conditions. Since enolase is essential under anaerobic conditions, we wondered whether enolase bound to RNase E/degradosomes plays a role in anaerobically induced cell filamentation. We generated another strain (Rned823–850) in which the chromosome region encoding amino acid residues 823–850 of RNase E [constituting the RNase E microdomain for enolase recognition (15)] was deleted. The Rned823–850 strain could host PNPase and RhlB helicase, but not enolase, in degradosomes under both aerobic and anaerobic growth conditions (Fig. 2*B*, lanes 3 and 4). Like Rned500–1061, Rned823–850 exhibited a rod-shaped morphology under anaerobic conditions (Fig. 2 *A*, *e* and *f*). The growth rate of Rned823–850 was similar to that of MG1655 under aerobic conditions (Fig. S2*B*), but under anaerobic conditions Rned823–850 grew faster than MG1655 (Fig. S2*B*).

We generated a control strain, Rned984–1011, in which the chromosome region encoding amino acid residues 984–1,011 of RNase E was deleted (*SI Materials and Methods* and Fig. S4). This region does not interfere with degradosome formation, and the protein ratios of RNase E, PNPase, enolase, and RhlB in degradosomes of this strain have a stoichiometry similar to that of the MG1655 strain (Fig. 2*B*, compare lanes 1 and 2 with lanes 5 and 6). Like the MG1655 strain, strain Rned984–1011 had a filamentous morphology under anaerobic conditions (Fig. 2 *A*, *g* and *h*). The growth rate of Rned984–1011 was similar to that of MG1655 under

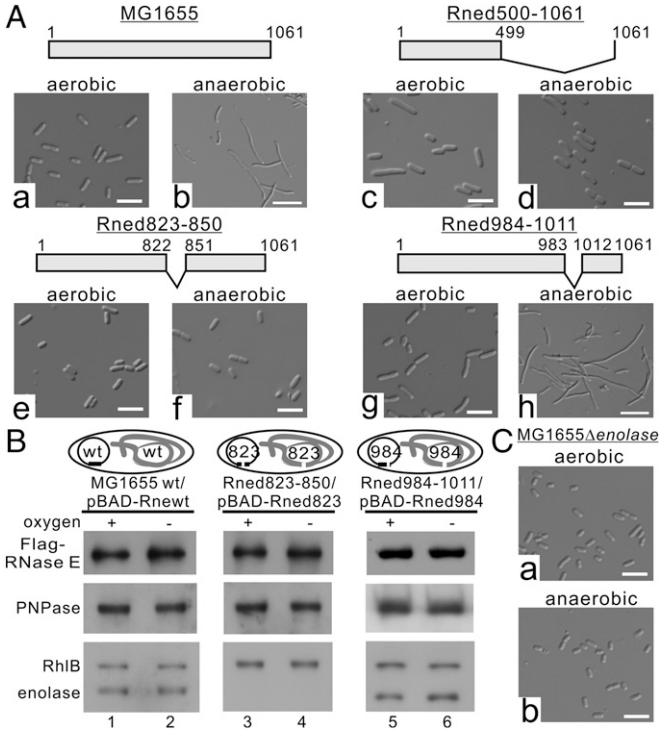

Fig. 2. Cell filamentation under anaerobic conditions requires enolase binding to RNA degradosomes. (*A*) Cell morphology of *E. coli* MG1655 (*a* and *b*) and its derivative strains (*c*–*h*) under aerobic and anaerobic conditions. Schematic representations of RNase E and its endogenous (untagged) and plasmid-encoded (Flag-tagged) variants are presented above the respective images. (Scale bars, 5 μm.) (*B*) The degradosomes isolated from *E. coli* MG1655 and its derivatives, Rned823–500 and Rne984–1011. Protein aliquots containing equal amounts of Flag-RNase E and its variants were analyzed by SDS/PAGE and immunoblotted with the indicated antibodies. Schematic representations of RNase E and its endogenous (untagged) and plasmid-encoded (Flag-tagged) variants are presented above the respective images. (*C*) Cell morphology of the *E. coli* MG1655Δenolase mutant with endogenously deleted enolase under aerobic and anaerobic conditions. (Scale bars, 5 μm.)

aerobic and anaerobic conditions (Fig. S2*A*), indicating that the deletion of residues 984–1,011 had no effect on cell growth.

Since enolase is essential under anaerobic conditions to sustain bacterial growth using glucose as a carbon source but not using other carbon sources such as pyruvate, glycerate, or succinate, we performed a reciprocal experiment using a strain deleted for the *eno* gene (i.e., without enolase), grown with pyruvate-supplemented minimal medium, to address whether enolase is required for RNase E/degradosome anaerobically induced cell filamentation. This strain, MG1655Δ*eno*, has intact full-length RNase E but lacks enolase and has a rod-shaped morphology, similar to the Rned500–1061 or Rned823–850 strains (Fig. 2*C*). Together, these data demonstrate that the filamentous morphology under anaerobic conditions requires enolase-bound RNA degradosomes.

Filamentous Cells Induced by Oxygen-Limited Conditions Have Limited Septum Formation and Decreased FtsZ Protein Expression Levels. The filamentous morphology suggests limited septum formation under anaerobic conditions. Septum formation in *E. coli* begins by assembling three essential proteins—FtsZ, FtsA, and ZipA—to form a proto-ring attached to the midcell inner membrane (see ref. 16 for a review). As shown in Fig. 3*A*, FtsZ protein levels were significantly decreased in *E. coli* MG1655 under anaerobic conditions (in contrast, no difference in FtsA and ZipA protein levels was observed), suggesting that FtsZ total enzymatic activity is lower under anaerobic than in aerobic conditions. *E. coli* MG1655 also exhibited a limited capability for septum formation under anaerobic conditions (Fig. 3*D*), as is consistent with the reduced FtsZ levels. We confirmed that protein stability and abundance of *ftsZ* mRNA were equivalent under both aerobic and anaerobic conditions (Fig. 3 *B* and *C*). Therefore, anaerobic conditions result in the inhibition of FtsZ protein synthesis at the posttranscriptional level.

Both the sRNA DicF and Hfq Are Necessary to Reduce FtsZ Protein Levels and Induce Cell Filamentation Under Anaerobic Growth Conditions. The sRNA DicF is responsible for decreased FtsZ protein levels through translational inhibition (17–19), so deletion of sRNA DicF should reveal a rod-shaped cell morphology in *E. coli* MG1655 under anaerobic conditions. Therefore, we analyzed the cell morphology of an endogenously deleted *dicF* strain, MG1655Δ*dicF* (20), under aerobic and anaerobic conditions. This strain exhibited a rod-shaped morphology (cell length ~2.0–2.5 μm) (Fig. 3 *E*, *a* and *b*) under both aerobic and anaerobic conditions, and, tellingly, its FtsZ protein levels were unchanged under anaerobic conditions (Fig. 3*G*, lanes 1 and 2). The growth rate of MG1655Δ*dicF* was similar to that of MG1655 under aerobic conditions (Fig. S2*C*), but under anaerobic conditions MG1655Δ*dicF* grew faster than MG1655 (Fig. S2*C*), and its growth rate was similar to that of the Rned823–850 strain (compare Fig. S2 *B* and *C*).

Given that sRNA DicF is a known inhibitor of FtsZ (21), we first ectopically expressed sRNA DicF (53 nt) in MG1655Δ*dicF* using an arabinose-inducible promoter from the pBAD plasmid and observed that cells became filamentous aerobically (Fig. S5*A*). As in aerobically induced filamentation, cells regained their filamentous shape (cell length >5 μm) (Fig. 3 *E*, *c*), and FtsZ protein levels were reduced (Fig. 3*G*, lanes 3 and 4) following ectopic expression of sRNA DicF under anaerobic conditions. This aerobically or anaerobically induced filamentation by sRNA DicF overexpression was also observed in Rned823–850 cells (Fig. S5*B*), so it is not dependent upon the enolase-binding site in RNase E.

Many *trans*-encoded sRNAs, including DicF, require the chaperone protein Hfq for their stability and base-pairing activity under aerobic growth conditions (22–24). Hfq action on sRNA stability and function may also happen under anaerobic conditions. If so, deletion of the *hfq* gene should destabilize DicF and produce similar FtsZ protein levels under both aerobic and anaerobic conditions, and the cells should have a rod-shaped cell morphology under anaerobic conditions. Indeed, our MG1655Δ*hfq* strain was rod-shaped (Fig. 3 *F*, *a* and *b*) under anaerobic conditions, and its FtsZ protein levels were similar under both aerobic and anaerobic conditions (Fig. 3*H*, lanes 1 and 2). MG1655Δ*hfq* grew slightly more slowly than MG1655 (Fig. S2*D*) under aerobic conditions. However, under anaerobic conditions, MG1655Δ*hfq* grew faster than MG1655 cells (Fig. S2*D*). In the MG1655Δ*hfq* strain with ectopically expressed Hfq by the arabinose-inducible promoter, the cells again became filamentous under anaerobic conditions (cell length >5 μm) (Fig. 3 *F*, *c*), and FtsZ protein levels were reduced (Fig. 3*H*, lanes 3 and 4).

Thus, our results show that both sRNA DicF and the RNA chaperone Hfq are required for the filamentous transition of *E. coli* under anaerobic conditions. Since the level of FtsZ decreases under anaerobic conditions, it could be assumed that the level of its negative regulator, sRNA DicF, increases under the same conditions.

53-nt sRNA DicF Accumulates Under Anaerobic Conditions. Pre-DicF RNA was transcribed from the *dicA-ydfABC-dicF* operon, and the transcript (~850 nt long) was further processed by RNaseIII and RNase E via intermediate fragments (18) into mature 53-nt sRNA DicF. However, the processing steps to produce the mature sRNA are still unknown. Instead of using a strain deleted for *dicF* (as in Fig. 3)—namely, the MG1655Δ*dicF* mutant carrying the *dicA-ydfABC-*Δ*dicF* operon, which produces a truncated transcript with

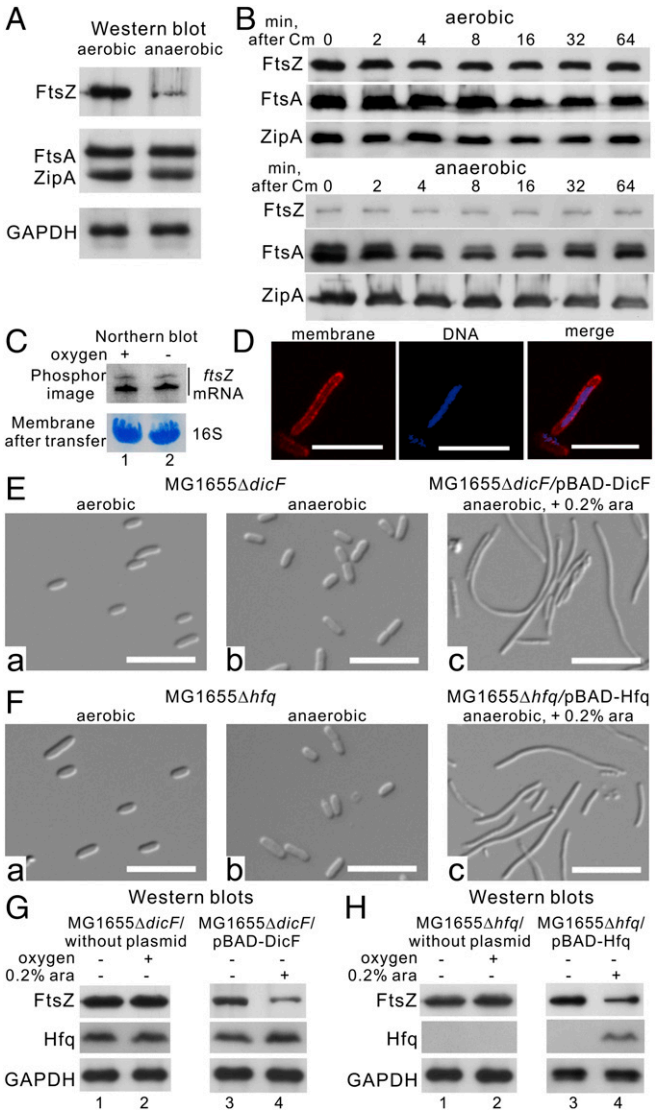

Fig. 3. Both sRNA DicF and Hfq are necessary to reduce FtsZ protein levels, leading to cell filamentation under anaerobic conditions. (*A*) FtsZ, FtsA, and ZipA endogenous protein levels under aerobic and anaerobic conditions. Whole-cell extracts were analyzed by SDS/PAGE and immunoblotted with the indicated antibodies. (*B*) FtsZ, FtsA, and ZipA protein stability under both aerobic and anaerobic conditions. Cells were collected at the indicated times (0, 2, 4, 8, 16, 32, and 64 min) after chloramphenicol (Cm) treatment, lysed, and assayed by Western blotting. The bands corresponding to endogenous FtsZ, FtsA, and ZipA are indicated. (*C*) *ftsZ* mRNA steady-state levels under aerobic and anaerobic conditions. The bands corresponding to endogenous *ftsZ* mRNA (Northern blot) and 16S ribosomal RNA (membrane after transfer) are indicated. (*D*) Fluorescence images of anaerobically induced filamentous cells. Membrane (red) and DNA (blue) were visualized by FM 4-64 and Hoechst 33342 dyes, respectively. (*E*, *a* and *b* and *F*, *a* and *b*) Cell morphology of the MG1655Δ*dicF* and MG1655Δ*hfq* mutants under aerobic and anaerobic conditions. (Scale bars, 5 μm.) (*E*, *c* and *F*, *c*) Cell morphology of the MG1655Δ*dicF* and MG1655Δ*hfq* mutants after arabinose-induced expression of sRNA DicF (*E*, *c*) or Hfq (*F*, *c*), respectively, under anaerobic conditions. (Scale bars, 5 μm.) (*G* and *H*) Western blot analysis of the MG1655Δ*dicF* (*G*) and MG1655Δ*hfq* (*H*) mutants under aerobic and anaerobic conditions and after arabinose-induced expression of sRNA DicF or Hfq under anaerobic conditions. The bands corresponding to endogenous FtsZ, Hfq, and GAPDH and ectopically expressed Hfq are indicated.

an unknown RNA secondary structure—we used a strain without the operon as a negative control to precisely identify pre-DicF–specific transcripts, intermediate RNA, and mature RNA products in the MG1655 strain by Northern blot analyses. To identify a strain lacking the entire *dicA-ydfABC-dicF* operon in its genome for use as a negative control for Northern blots, we conducted in silico analysis of *E. coli* genomes using the BioCyc Database Collection (https://biocyc.org). Interestingly, most commensal strains lack *dicF* in their genomes. In contrast, pathogenic *E. coli* strains have multiple copies of *dicF* (Fig. 4*B* and Table S1). In this study, we used *E. coli* Nissle 1917 as a negative control to identify the DicF-specific hybridization signal(s). We performed Northern blot analyses using two specific probes for the detection of sRNA DicF and its precursor RNA transcribed from the *dicA-ydfABC-dicF* operon (Fig. 4*A*) and compared the RNA steady-state levels under aerobic and anaerobic conditions in *E. coli* MG1655. Using internal radiolabeled antisense RNA probe 1 (Fig. 4*A*), we detected specific upper (~183-nt) and lower (~130-nt) bands (indicated by asterisks in Fig. 4 *C*, *a*, lanes 1 and 2) that were not present in the *E. coli* Nissle 1917 strain (Fig. 4 *C*, *a*, lanes 3 and 4). Using antisense RNA probe 2 (Fig. 4*A*), we detected several specific bands not present in the *E. coli* Nissle 1917 strain (indicated by arrowheads in Fig. 4 *C*, *b*; compare lanes 1 and 2 with lanes 3 and 4), one of which was the same upper band [~183 nt; a product of RNase III processing (18)] detected by probe 1; the others were lower bands (~50 nt) (Fig. 4 *C*, *b*, lanes 1 and 2). The upper band (~183 nt) detected by both probes represented the 183-nt RNA precursor of sRNA DicF (which we refer to as "DicF precursor"), and the lower band (~130 nt) detected only by probe 1 but not by probe 2 was the 130-nt 5′-upstream intermediate product arising from RNase E cleavage of the DicF precursor (which we refer to as the "130-nt product") (Fig. 4*A*). The other RNase E cleavage products detected at the 3′ end of the DicF precursor, which were detected by probe 2 but not by probe 1, are variants of the 53-nt sRNA DicF (referred to as "53-nt DicF") and/or its degradation products, represented by the multiple lower bands in Fig. 4 *C*, *b*.

To determine whether sRNA DicF is preferentially enriched under anaerobic conditions, we probed another Hfq-dependent Spot42 sRNA (25), which plays essential roles as a regulator of carbohydrate metabolism and uptake and expression of which is activated by glucose (26), and found that steady-state levels of the RNA decreased, rather than increased like DicF, under anaerobic conditions (Fig. 4 *C*, *c*). This result indicates that sRNA DicF is preferentially enriched under anaerobic conditions.

Although 53-nt DicF predominantly accumulated under oxygen-limited conditions (Fig. 4 *C*, *b*, lane 2), neither it nor its variants were detected in the MG1655Δ*hfq* strain under either aerobic or anaerobic conditions (Fig. 4 *D*). This observation was expected, as Hfq specifically protects sRNA DicF from degradation under normal growth conditions (27); in the absence of Hfq, 53-nt DicF and its derivatives were rapidly cleaved and thus were not detected.

RNA Cleavage by RNase E Is Oxygen Responsive and Is Necessary for Cell Filamentation Under Oxygen-Limited Conditions. Since 53-nt DicF accumulated under oxygen-limited conditions, we performed a Northern blot to determine the impact of oxygen levels on 53-nt DicF. Under aerobic–anaerobic–aerobic alternating growth conditions, 53-nt DicF and its precursor accumulated after shifting to anaerobiosis and then reverted to their original state after shifting back to aerobic conditions (Fig. 4*E*, compare lanes t0 and t1 with lanes t2 and t3 and with t4–t6, respectively, and Fig. S5*D*). We detected a similar pattern for the 130-nt product.

We then investigated whether RNase E is responsible for DicF precursor cleavage and production of the 130-nt and 53-nt DicF cleavage products. We used the RNase E temperature-sensitive strain N3431 (28), in which RNase E activity is inhibited under nonpermissive temperatures, since the DicF precursor should accumulate in the N3431 cells under nonpermissive temperatures. As shown in Fig. 4*F*, we found that after shifting to a nonpermissive temperature (44 °C) for 3 h, levels of the DicF precursor increased significantly compared with 30 °C (detected by

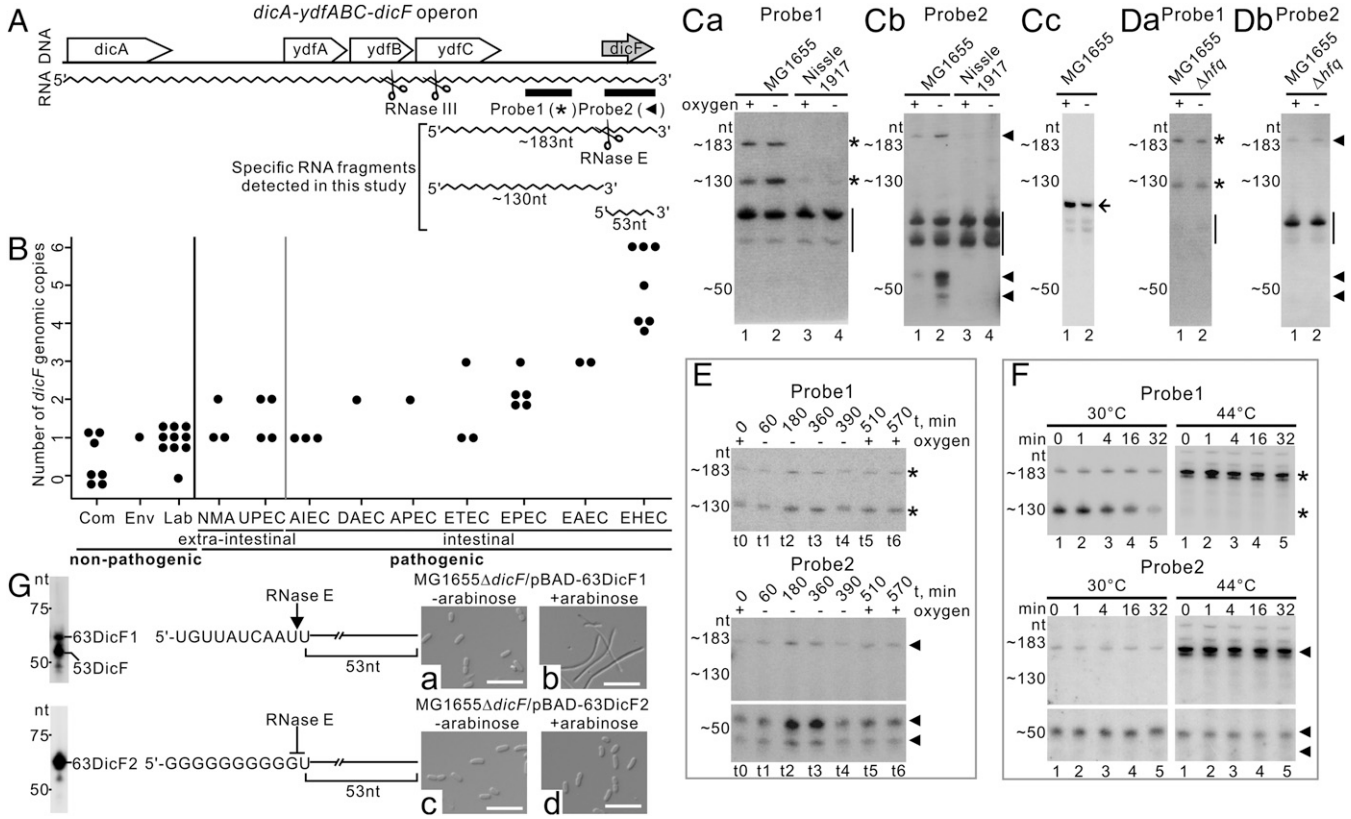

Fig. 4. DicF RNA levels are oxygen responsive, and DicF production (processing) and decay (degradation) depend on RNase E. (*A*) Schematic representation of the *dicA-ydfABC-dicF* operon with RNase III and RNase E cleavage sites (modified from ref. 18). Probes 1 (*) and 2 (◄) for Northern blots and the specific RNA fragments detected in this study are indicated. (*B*) Number of *dicF* genomic copies in nonpathogenic *E. coli* strains (Com, commensal; Env, environmental; Lab, laboratory) and pathogenic (AIEC, adherent-invasive; APEC, avian pathogenic; DAEC, diffusely adhering; EAEC, enteroaggregative; EHEC, enterohemorrhagic; EPEC, entheropathogenic; ETEC, enterotoxigenic; NMA, neonatal meningitis-associated; UPEC, uropathogenic). Each dot represents one *E. coli* strain. (*C*, *a* and *b* and *D*) Northern blot analyses of sRNA DicF in *E. coli* MG1655 (*C*) and in the MG1655Δ*hfq* mutant (*D*) under aerobic and anaerobic conditions. Specific signals of probe 1 (*), probe 2 (◄), and nonspecific signals (black solid lines) are indicated at the right of each gel. (*C*, *c*) Northern blot analysis of sRNA Spot42 in *E. coli* MG1655 under aerobic and anaerobic conditions. Specific signal is indicated by a black arrow at the right of the gel. (*E*) DicF RNA levels under aerobic–anaerobic–aerobic alternating growth conditions. Specific signals of probe 1 (*) and probe 2 (◄) are indicated. (*F*) RNA stability of DicF, 130-nt product, or DicF precursor in the *E. coli* temperature-sensitive N3431 strain grown anaerobically at permissive (30 °C) and nonpermissive (44 °C) temperatures. Equal amounts of total RNA extracted from the cells before and after rifampicin treatment at the times indicated were analyzed by Northern blotting using probe 1 (*) and probe 2 (◄). (*G*, *Right*) Cell morphologies of *E. coli* MG1655Δ*dicF* before and after ectopic expression of the 63DicF1 DicF miniprecursor or a 63DicF2 variant under anaerobic conditions. (Scale bars, 5 μm.) (*Left*) Northern blots upon arabinose ectopic expression under anaerobic conditions are shown. (*Center*) Schematic representations of the 63DicF1 DicF miniprecursor and the 63DicF2 variant and their RNase E cleavage sites.

both probes 1 and 2) (Fig. 4*F*, compare lane 1 under 44 °C vs. 30 °C). The 130-nt product was not produced at 44 °C but was detected at 30 °C (probe 1) (Fig. 4*F*, compare lane 1 under 44 °C vs. 30 °C). As expected, at 44 °C, levels of 53-nt DicF were comparable to those at 30 °C (probe 2) (Fig. 4*F*, *Lower*; compare lane 1 under 44 °C vs. 30 °C). In fact, 53-nt DicF was slowly degraded at both 30 °C and 44 °C (probe 2) (Fig. 4*F*, compare lanes 1–5 in the left and right panels). In contrast to 53-nt DicF, the 130-nt product was less stable ($t_{1/2}$ ~17 min at 30 °C) at permissive temperatures and was completely degraded after shifting to the 44 °C nonpermissive temperature for 3 h (probe 1) (Fig. 4*F*, compare lanes 1–5 in the left and right panels). Thus, our data indicate that RNase E is necessary for cleavage of the DicF precursor to produce the 130-nt product and 53-nt DicF and that degradation of the 53-nt DicF, but not the 130-nt product, is predominantly dependent on RNase E activity.

Since Hfq protects 53-nt DicF from degradation, and both Hfq and 53-nt DicF are necessary for cell filamentation under anaerobic conditions, we examined whether RNase E cleavage of the DicF precursor to generate 53-nt DicF is required for cell filamentation under anaerobic conditions. We introduced an arabinose-inducible pBAD-plasmid—expressed either as a 63DicF1 DicF miniprecursor containing the 53-nt sRNA DicF plus a 10-nt wild-type upstream region with an RNase E cleavage site (so it could be cleaved by RNase E) or a 63DicF2 variant in which the RNase E cleavage site had been replaced by 10 guanines in the 53-nt DicF upstream region (so it could not be cleaved by RNase E), as described in *SI Materials and Methods*. Unlike 63DicF1, 63DicF2 was not cleaved by RNase E under either anaerobic or aerobic conditions (left panels in Fig. 4*G* and Fig. S5*C*, respectively). As a result, in contrast to the 63DicF2 variant (Fig. 4 *G*, *c* and *d* and Fig. S5 *C*, *c* and *d*), a filamentous cell morphology was obtained for MG1655Δ*dicF* only upon expression of the 63DicF1 miniprecursor under anaerobic or aerobic conditions (Fig. 4 *G*, *a* and *b*, and Fig. S5 *C*, *a* and *b*, respectively). Our data demonstrate that RNase E cleavage (processing) is a necessary step for the production of functional 53-nt sRNA DicF that induces cell filamentation under anaerobic conditions.

Enolase in the Degradosome Stabilizes 53-nt sRNA DicF Under Anaerobic Conditions. As shown in Fig. 2*A*, the MG1655 strain containing enolase-bound degradosomes is able to form filamentous cells under anaerobic conditions when functional 53-nt DicF accumulates. In contrast, the Rned823–850 strain containing enolase-free degradosomes lost the ability to form filamentous

cells under the same conditions, suggesting that 53-nt DicF levels in this strain are not comparable to those in the MG1655 strain.

Northern blot analyses were performed to determine RNA abundances of 53-nt DicF, its precursor, and the 130-nt product in the MG1655, Rned984–1011, and Rned823–850 strains at different time points after rifampicin treatment under aerobic and anaerobic conditions. We found that the abundance and stability of all RNA species were relatively similar in all three strains under aerobic conditions (probes 1 and 2) (Fig. 5*A*, compare lanes 1–5, 6–10, and 11–15, respectively). In contrast, under anaerobic conditions, the abundance and stability of 53-nt DicF and the 183-nt precursor were lower for Rned823–850 than for the MG1655 and Rned984–1011 strains (probes 1 and 2) (Fig. 5*B*, compare lanes 11–15, 1–5, and 6–10, respectively). The RNA steady-state levels of the 130-nt product were similar under both aerobic and anaerobic conditions. However, its degradation rate was greater in Rned823–850 than in the MG1655 and Rned984–1011 strains under anaerobic conditions (Fig. 5*B*, compare lanes 11–15, 1–5, and 6–10, respectively). Our data show that disruption of the enolase and RNase E interaction results in faster degradation of the 130-nt product ($t_{1/2}$ ~12 min in Rned823–850 vs. $t_{1/2}$ >32 min in MG1655) and 53-nt DicF under anaerobic conditions ($t_{1/2}$ ~17 min in Rned823–850 vs. $t_{1/2}$ >32 min in MG1655) (Fig. S5*E*).

We used sRNA Spot42 again to monitor RNA half-life by Northern blot analysis. We found that Spot42 sRNA half-life is not changed under either aerobic or anaerobic conditions in all strains: MG1655, Rned823–850, and Rned984–1011 (Fig. 5 *C* and *D*). The data show that RNA turnover of Spot42 is not affected by deletion of the enolase-binding microdomain in RNase E. Thus, the anaerobically induced faster degradation of the sRNA DicF by the nonenolasic degradosomes in the Rned823–850 strain is specific. Collectively, our data show that the enolase association specifically helps stabilize DicF (and, possibly, its processing) but not Spot42 sRNA under anaerobic conditions.

Binding of Enolase to RNase E Does Affect Protein Levels and Impacts Subcellular Localization of RNase E Under Anaerobic Conditions. The fast turnover of the DicF precursor under anaerobic conditions in the Rned823–850 strain that lacks enolase in degradosomes could be caused by increased RNase E protein levels. Therefore, we determined the protein levels of RNase E/RNase E variants in the MG1655, Rned823–850, and Rned984–1011 strains under both aerobic and anaerobic conditions. We found that for all three strains the levels of RNase E or its derivative protein were reduced under anaerobic conditions (Fig. 6*A*). Quantitation indicated that RNase E protein levels decreased to a lesser extent under anaerobic conditions in the Rned823–850 mutant (~2.5-fold) than in the MG1655 (~4.0-fold) or Rned984–1011 (~3.4-fold) strains.

Previous studies have shown that RNase E–degradosome complexes are tethered to the cytoplasmic membrane in vivo (5) and that membrane-binding of the RNase E N terminus (which contains a catalytic domain) stabilizes protein structure and increases both RNA cleavage activity and substrate affinity (6). We investigated whether binding of enolase to RNase E may change the subcellular localization of RNase E under anaerobic conditions and thereby regulate protein stability and enzymatic activity and stabilize functional sRNA DicF in the MG1655 and Rned984–1011 strains. We used EvoGlow fluorescent reporter protein to study the subcellular localization of RNase E under aerobic and anaerobic conditions, as this fluorescent reporter can be detected under both conditions (29). We constructed MG1655 Rne-Bs1, Rned823–850-Bs1, and Rned984–1011-Bs1 strains in which the fluorescent reporter was fused to the chromosomal C terminus of RNase E through a polypeptide linker (*SI Materials and Methods*). Our results show that for the MG1655 or Rned984–1011 strains that host enolase in the degradosomes, the subcellular distribution

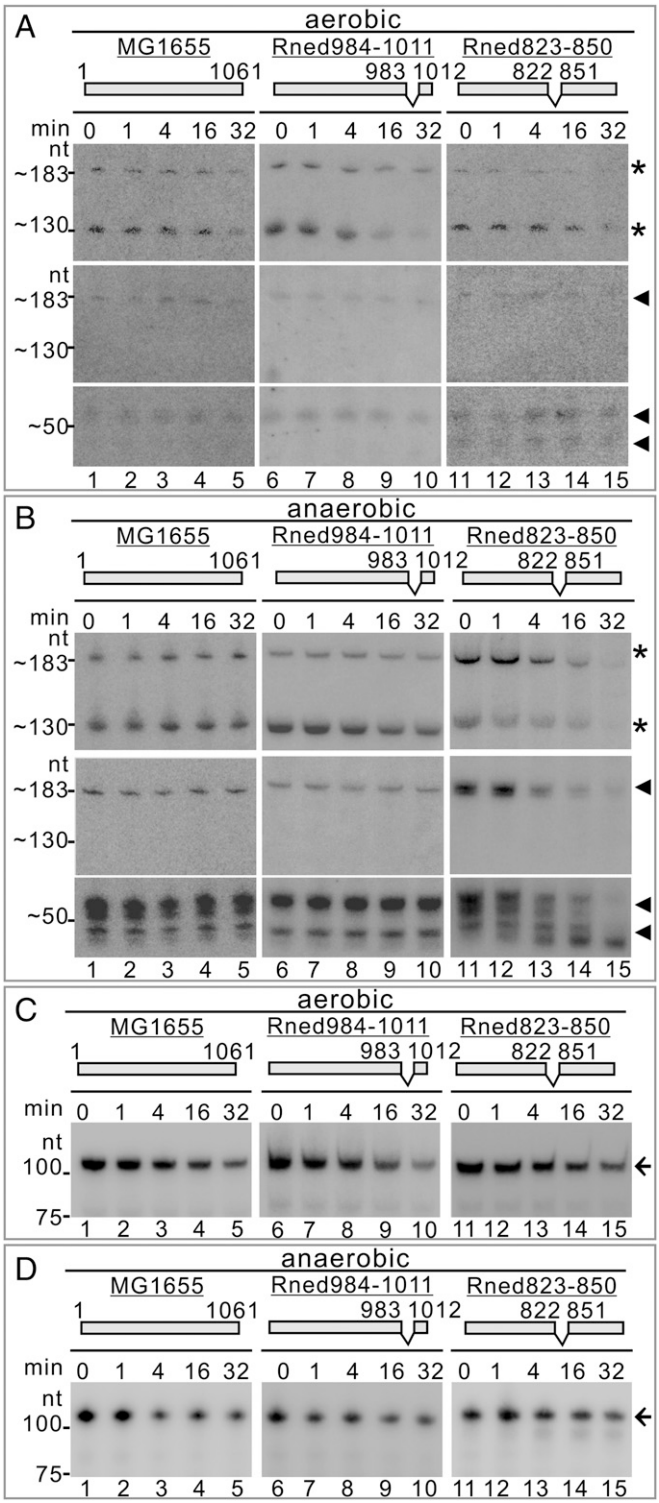

Fig. 5. DicF processing and degradation are dependent on enolase being bound to RNase E. (*A* and *B*) sRNA DicF RNA half-lives in the *E. coli* MG1655, Rned984–1011, and Rned823–850 strains under aerobic (*A*) and anaerobic (*B*) conditions. RNA samples prepared from the cultures before and after rifampicin treatment at the times indicated were analyzed by Northern blotting using probe 1 (*) and probe 2 (◄). (*C* and *D*) RNA half-lives of sRNA Spot42 in the *E. coli* MG1655, Rned984–1011, and Rned823–850 strains under aerobic (*C*) and anaerobic (*D*) conditions. Specific signals are indicated by black arrows on the right side of each gel.

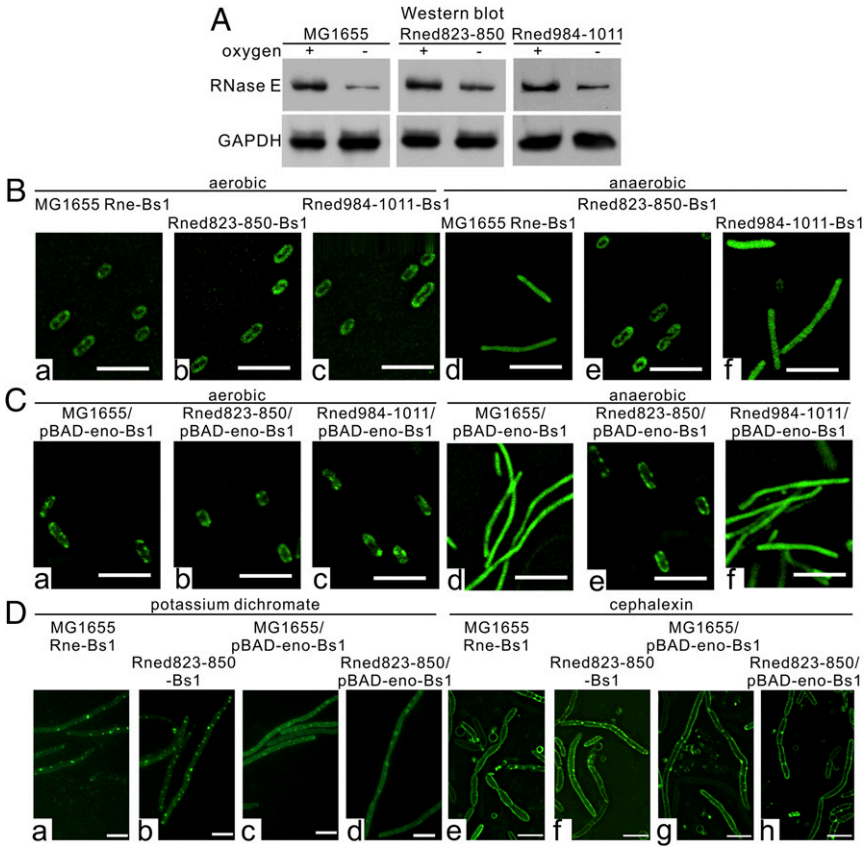

Fig. 6. The diffuse localization pattern of RNase E and enolase is specific to anaerobic conditions. (*A*) Endogenous expression levels of RNase E and its variants in the *E. coli* MG1655, Rned823–850, and Rned984–1011 strains under aerobic and anaerobic conditions. Whole-cell extracts were analyzed by SDS/PAGE and immunoblotted with the indicated antibodies. (*B* and *C*) Subcellular localization of RNase E and its variants (*B*) and enolase (*C*) under aerobic and anaerobic conditions in the *E. coli* MG1655, Rned823–850, and Rned984–1011 strains. (Scale bars, 5 μm.) (*D*) Subcellular localization of RNase E and its variant lacking the enolase-binding microdomain and enolase upon potassium dichromate (*D*, *a*–*d*) and cephalexin (*D*, *e*–*h*) treatments in the *E. coli* MG1655 and Rned823–850 strains under aerobic conditions. (Scale bars, 5 μm.)

of RNase E shifted from the cytoplasmic membrane under aerobic conditions to a diffuse pattern under anaerobic conditions (Fig. 6 *B*, *a*, *d* and *c*, and *f*, respectively). However, for the Rned823–850 strain, whose degradosomes lacked enolase, RNase E was cytoplasmic membrane-associated under both conditions (Fig. 6 *B*, *b* and *e*). Furthermore, our results show that whenever RNase E was tethered to the cytoplasmic membrane of MG1655 (Fig. 6 *B*, *a*), Rned823–850 (Fig. 6 *B*, *b*), or Rned984–1011 (Fig. 6 *B*, *c*) cells under aerobic conditions or of Rned823–850 (Fig. 6 *B*, *e*) cells under anaerobic conditions, 53-nt DicF turnover was rapid, whether or not enolase was hosted by the degradosomes. In agreement with this idea that association with the cytoplasmic membrane increases RNase E enzymatic activity, the Rned823–850 RNase E variant tethered to the cytoplasmic membrane under both aerobic and anaerobic conditions exhibited faster degradation of 53-nt DicF under both conditions (Figs. 5 *A* and *B*, lanes 11–15, and 6 *B*, *b* and *e*). When RNase E binds to enolase and is diffuse in the cytoplasm (under anaerobic conditions), and thus is not tethered to the cytoplasmic membrane (as it is under aerobic conditions), this may lock RNase E into a less active conformation for sRNA degradation, thereby stabilizing sRNA DicF.

To examine whether the diffuse localization pattern of RNase E and enolase is specific to anaerobically induced filamentous cells, we used other means of inducing cell filamentation under aerobic conditions (i.e., potassium dichromate and cephalexin). We found that the localization patterns of RNase E and enolase under these conditions (Fig. 6*D*) differed from those under anaerobiosis (Fig. 6 *B* and *C*). The pattern under potassium dichromate and cephalexin treatment is not affected by nonenolasic degradosomes (Fig. 6*D*, compare *a* and *b* with *e* and *f*). Thus, the diffused localization pattern of RNase E and enolase (Fig. 6 *B*, *d* and Fig. 6 *C*, *d*, respectively) is specific to anaerobically induced filamentous cells, and the localization pattern depends on how filamentation is induced (i.e., by low oxygen or potassium dichromate/cephalexin treatment).

To understand whether RNase E amounts affect the localization, we ectopically expressed RNase E fused with Bs1 protein using an arabinose-inducible promoter from the pBAD plasmid in the MG1655 Rne-Bs1 strain under anaerobic conditions and found that, upon low (namely, without ectopic expression) or increased (namely, after ectopic expression by arabinose) levels, RNase E has a similar diffused subcellular distribution (Fig. S6*A*). Thus, the decrease in RNase E amounts does not affect the localization pattern.

Collectively, our data demonstrate that under oxygen-limited conditions, enolase (in bound form to RNase E in the degradosome) is required for the filamentous transition of *E. coli* through its regulation of the subcellular localization, protein stability, and activity of RNase E.

Discussion

RNase E Enzymatic Activity and *E. coli* Cell Morphology. A previous study (28) showed that strains carrying the *me-3071* mutation, which renders activity of RNase E thermolabile, fail to divide and grow as filaments at the nonpermissive temperature of 43 °C. Some filaments grew as big as 12 μm and contained up to four constriction

sites. Over 75% of the filaments appeared to have at least one incomplete septum. Thus, it appears that the loss of RNase E activity is responsible for an early loss of the cell's capacity to divide. In that study, the *E. coli* cells stopped cell growth/division nearly 3 h after being shifted to the nonpermissive temperature, but growth resumed when the culture was shifted back to 37 °C. In contrast, the anaerobically induced filamentous cells in our study are viable and continue to grow under anaerobic conditions. These cells have the ability to accumulate cell biomass under anaerobic conditions. Anaerobically induced cell filamentation was reversible, and the MG1655 strain reverted to a rod-shape morphology within ~3 h after being returned to aerobic conditions (Fig. 1 *D*, *b*).

Although the absence of RNase E is lethal, the *rne*-deletion strain can be made viable by RNase G overexpression. Filamentous morphology was observed during culture in liquid medium under normal growth conditions in the KSL2000 strain, in which a chromosomal deletion in *rne* was complemented by a plasmid-borne *rng* gene under the control of an arabinose gene promoter (30). This filamentous morphology was completely reversed by complementation with full-length RNase E (30). We found that ectopic expression of RNase E also induced reversion to a rod-shaped morphology under anaerobic conditions (Fig. 1 *E*, *a* and *b*). Thus, RNase E enzymatic activity clearly has a role in determining *E. coli* cell morphology under both conditions. However, in the *rne* temperature-sensitive strain N3431 the levels of 53-nt DicF are very low (almost undetectable) under both permissive and nonpermissive temperatures (Fig. S5*F*), and the functional role of such a low level of sRNA under these conditions is therefore probably negligible.

Regulation of RNase E Activity. Activity of RNase E can be regulated by inhibitors such as RraA, RraB (10), and ribosomal protein L4 (11). Previously, we found that RNase E associated with a membrane has increased enzymatic activity and substrate affinity (6), suggesting that compartmentation of RNase E plays a role in regulating its enzymatic activity in vivo. Moreover, here we have shown that RNase E has different subcellular distributions in the MG1655 and Rned984–1011 derivative strains. RNase E distribution depends on the presence or absence of oxygen, with the enzyme being tethered to the cytoplasmic membrane under aerobic conditions or being distributed in the cytoplasm under anaerobic conditions. We also found that RNA turnover and cleavage of the DicF precursor were faster under aerobic conditions than under anaerobic conditions in the MG1655 and Rned984–1011 strains. This result is consistent with the idea that RNase E substrate specificity/activity is differentially regulated by its subcellular distribution in the cell.

Enolasic RNA Degradosomes Are Necessary for Anaerobic-Responsive DicF RNA Degradation. We have shown that enolase alters the subcellular localization of RNase E from the cytoplasmic membrane to diffuse patterns when it binds to the RNase E scaffolding region (Fig. 6*B*) and that cells became filamentous under anaerobic conditions (Fig. 1 *B*, *a* and *b*). Our findings also suggest that degradation of certain RNA species, such as sRNA DicF, takes place near the membrane and depends on high RNase E activity. Other RNAs found in the cytoplasm do not require high RNase E activity for their degradation. Although the deletion of the enolase-binding site on RNase E does not affect the association of Hfq with RNase E (Fig. S6*B*), we cannot exclude other possibilities, such as a mechanism by which Hfq protects sRNA from degradation that is differentially regulated by some unknown mechanism(s) related to RNase E or sRNA subcellular distributions.

RNase E degradosomes have been shown to be tethered to the cytoplasmic membrane by the N-terminal region of RNase E (amino acids 1–602) (5). Subsequently, an RNase E region (segment A; amino acids 562–587) that was proposed to have the propensity to form an amphipathic α-helix was found to be required for RNase E binding to cytoplasmic membranes (31). Recently, it was found that the N-terminal 499-aa residues of RNase E (NRne) interact with the cytoplasmic membrane through electrostatic interactions (6). NRne membrane-binding induces a structural change in NRne that may lead to a flexible protein conformation (6). In this study, we show that the subcellular membrane distribution of RNase E is the same in the MG1655 Rne-Bs1, Rned823–850-Bs1, and Rned984–1011-Bs1 variants under aerobic conditions, which indicates that the conformation of these RNase E derivatives is not altered. In contrast, the subcellular RNase E distribution is altered (to a diffuse pattern) under anaerobic conditions in the MG1655 Rne-Bs1 and Rned984–1011-Bs1 strains but not in Rned823–850, suggesting that the physical interaction of RNase E with enolase changes the protein conformation under those conditions, leading to an altered subcellular distribution of RNase E.

Enolase from the anaerobic Gram-negative bacterium *Bacteroides fragilis*, frequently found in intestines and known to cause intraabdominal infections, was found to be a heme-binding protein (32). It has been speculated that the original evolutionary function of hemoproteins was electron transfer in ancestral

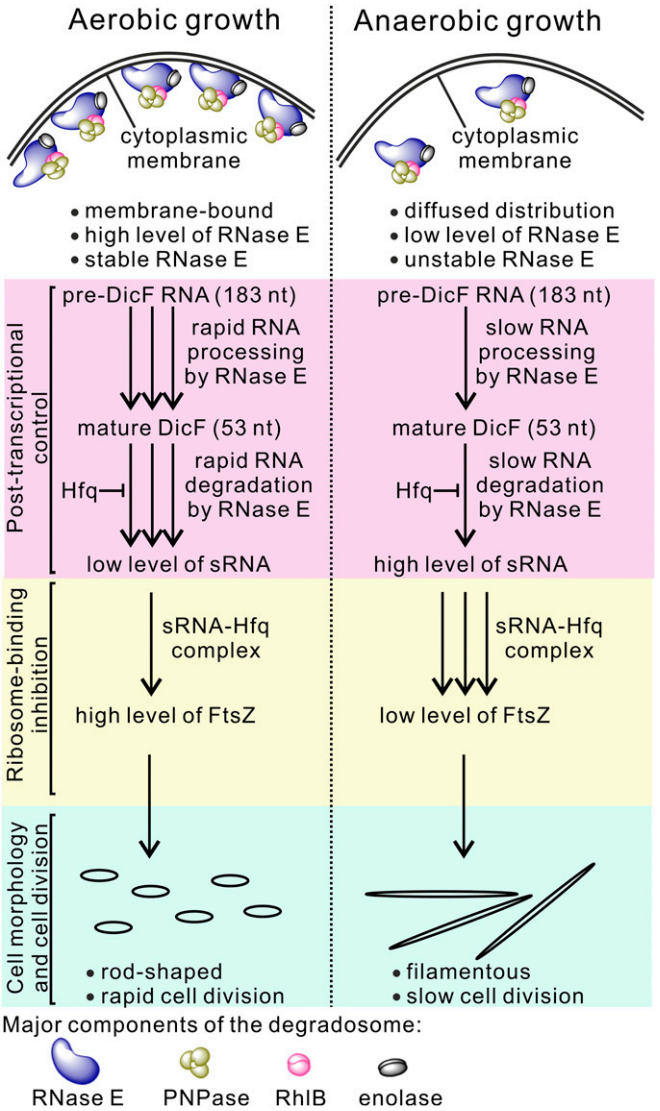

Fig. 7. RNase E, enolasic degradosomes, and sRNA mediate the regulation of cell shape and division. Growth conditions, the components of degradosomes, and what happens when the bacteria are under aerobic or anaerobic conditions are shown.

cyanobacteria-like organisms before the appearance of molecular oxygen (33). Upon binding of a diatomic gas, such as O_2, CO, or NO, heme undergoes conformational changes (34) that can induce conformational changes in its interacting partner protein (s). We hypothesize that enolase in the *E. coli* enolasic degradosome is a heme-binding protein and that the binding of the diatomic gas to the heme protein induces conformational changes in RNase E/degradosomes. As a result, RNase E/degradosome attachment or detachment from the membrane can be regulated in response to oxygen levels. Whether the RNase E inhibitors RraA, RraB, or L4 can change the subcellular localization of RNase E is unknown.

Enolase in the RNA degradosome has been reported to be involved in the rapid decay of glucose transporter *ptsG* mRNA under aerobic growth conditions (35). Bacteria should have different strategies to regulate RNA levels to adapt their metabolism and thereby survive in different conditions. We suggest that alteration of RNase E cleavage by enolase in the degradosome may depend on factors such as environmental growth conditions, substrate specificity, and substrate availability, which allow the degradosome to quickly target specific RNA species for degradation.

Functions of Enolase Outside Glycolytic Metabolism and Its Role in Anaerobically Induced Cell Filamentation. Enolase is primarily known for its role in glycolysis, a metabolic pathway involved in ATP and NADH production. It also plays a central role in metabolism by providing its intermediates to several other pathway processes (36). This metabolic pathway is particularly essential under anaerobic conditions. Enolase is essential for sustaining bacterial growth, with *E. coli* mutants with a disrupted *eno* gene being unable to grow without additional medium supplements such as pyruvate, glycerate, or succinate. It is known that other glycolytic enzymes, such as phosphoglucose isomerase and glyceraldehyde-3-phosphate dehydrogenase, exhibit other functions in addition to their major enzymatic activities in various organisms (37). We have shown that enolase has a degradosome-specific function and plays a role in altering RNase E cellular distribution/activity, resulting in cells having a filamentous shape under oxygen-limited conditions. The role of enolase in regulating sRNA degradation is another example of one of its multiple, so-called "moonlighting," functions. In addition, our data suggest that binding of enolase to the cytoplasmic membrane is independent of RNase E, and thus it probably has multiprotein partners on the membrane, such as the glycolytic complex (38).

Oxygen sensing is a fundamental biological process necessary for the adaptation of living organisms to variable habitats and physiological situations. One current model of oxygen sensing is based on a heme protein capable of reversibly binding oxygen (39). Since enolase from another anaerobic Gram-negative bacterium, *B. fragilis*, is a heme-binding protein (32), we hypothesize that *E. coli* enolase may be an oxygen-level sensor (see above).

Furthermore, structural analysis of enolase from the anaerobic protozoan *Entamoeba histolytica* indicates that it contains 2-PGA in the active site and exists in the open conformation; the Mg^{2+}(II) ion is absent from the active site (40). These studies also suggest that anaerobic conditions might change the conformation and oligomerization of *E. coli* enolase, as well as its ion-binding affinity, thereby altering the activity and function of the enzyme. Anaerobic conditions may also change the conformation of RNase E and major components of the degradosome such as RhlB helicase and PNPase and their enzymatic activities as well as the composition of the degradosome. These topics would be interesting avenues for future research.

Role of Cell Filamentation. Bacteria are the oldest organisms known, and, interestingly, the first bacteria had a filamentous morphology (41). At that time the Earth's atmosphere was almost without oxygen (42). Thus, a filamentous morphology was likely the first organismal form.

For many years, filamentous bacteria have been considered to be the overstressed, sick, and dying members of the population (43). More in-depth analyses have revealed that filamentous members of some communities have vital roles in the bacterial population's continued existence. Recently, filamentation has been implicated in bacterial survival during exposure to environmental stresses, which include host effectors, protist predators, and antimicrobial therapies (43). Differentiation into the filamentous form is also important for the survival of pathogenic bacteria (44–46). It remains unclear whether the molecular mechanisms that lead to filamentation are shared by these scenarios. In fact, there is evidence to suggest that multiple mechanisms are involved in the inhibition of septation that leads to filamentation. Our data provide a mechanism (Fig. 7) by which *E. coli* and perhaps other pathogenic bacteria can switch from a rod-shaped to the filamentous morphology that might be necessary for survival within host tissues and for virulence. The working model shows how RNase E, enolasic degradosomes, and sRNA regulate cell shape and division (limited septum formation) (Fig. 7). Authentic homologs of RNase E are found in many γ-proteobacteria such as *Yersinia pseudotuberculosis* (47) and *Vibrio angustum* (48), and their RNase E interacts with RhlB, enolase, and PNPase to form an RNA degradosome homologous (49) to the multienzyme complex in *E. coli*. We postulate that other facultative anaerobic and anaerobic bacteria possessing enolasic RNA degradosomes exhibit similar regulation of cell filamentation.

Materials and Methods

Bacterial Strains, Plasmids, and Growth Conditions. Strains, plasmids, and oligonucleotide sequences are in Tables S2–S4. Construction details and growth conditions are provided in *SI Materials and Methods*.

Additional materials and procedures are provided in *SI Materials and Methods*.

ACKNOWLEDGMENTS. We thank Dr. J. O'Brien and G. Cohen for help in editing the manuscript; Dr. K.-F. Chak (National Yang-Ming University) for the specific antibody for TolB; Prof. P. de Boer (Case Western Reserve University) for the specific antibodies for FtsA, FtsZ, and ZipA; W.-S. Wang (S.L.-C. laboratory) for the specific antibodies for Hfq; S.-P. Lee [Institute of Molecular Biology (IMB) Imaging Core Facility, Academia Sinica] for excellent technical support; Dr. J.-D. Huang (University of Hong Kong) for the MG1655*ΔdicF* strain; Dr. C.-H. Teng (National Cheng Kung University) for the *E. coli* Nissle1917 strain; and Dr. S.-M. Yu (IMB, Academia Sinica) for providing access to the Anaerobic System Glove Box. This work was supported by Grants 104-2311-B-001-011-MY3 from the Taiwan Ministry of Science and Technology (MOST) and by Grants AS 034006 and 022323 from Academia Sinica (to S.L.-C.). O.N.M. received MOST Postdoctoral Fellowships 104-2811-B-001-094 and 105-2811-B-001-094.

1. Mackie GA (2013) RNase E: At the interface of bacterial RNA processing and decay. *Nat Rev Microbiol* 11:45–57.
2. Kaberdin VR, et al. (1998) The endoribonucleolytic N-terminal half of Escherichia coli RNase E is evolutionarily conserved in Synechocystis sp. and other bacteria but not the C-terminal half, which is sufficient for degradosome assembly. *Proc Natl Acad Sci USA* 95:11637–11642.
3. Miczak A, Kaberdin VR, Wei CL, Lin-Chao S (1996) Proteins associated with RNase E in a multicomponent ribonucleolytic complex. *Proc Natl Acad Sci USA* 93:3865–3869.
4. Py B, Higgins CF, Krisch HM, Carpousis AJ (1996) A DEAD-box RNA helicase in the Escherichia coli RNA degradosome. *Nature* 381:169–172.
5. Liou GG, Jane WN, Cohen SN, Lin NS, Lin-Chao S (2001) RNA degradosomes exist in vivo in Escherichia coli as multicomponent complexes associated with the cytoplasmic membrane via the N-terminal region of ribonuclease E. *Proc Natl Acad Sci USA* 98: 63–68.
6. Murashko ON, Kaberdin VR, Lin-Chao S (2012) Membrane binding of Escherichia coli RNase E catalytic domain stabilizes protein structure and increases RNA substrate affinity. *Proc Natl Acad Sci USA* 109:7019–7024.
7. Bernstein JA, Khodursky AB, Lin PH, Lin-Chao S, Cohen SN (2002) Global analysis of mRNA decay and abundance in Escherichia coli at single-gene resolution using two-color fluorescent DNA microarrays. *Proc Natl Acad Sci USA* 99:9697–9702.

8. Bernstein JA, Lin PH, Cohen SN, Lin-Chao S (2004) Global analysis of Escherichia coli RNA degradosome function using DNA microarrays. *Proc Natl Acad Sci USA* 101: 2758–2763.
9. Tseng YT, Chiou NT, Gogiraju R, Lin-Chao S (2015) The protein interaction of RNA helicase B (RhlB) and polynucleotide phosphorylase (PNPase) Contributes to the homeostatic control of cysteine in Escherichia coli. *J Biol Chem* 290:29953–29963.
10. Gao J, et al. (2006) Differential modulation of E. coli mRNA abundance by inhibitory proteins that alter the composition of the degradosome. *Mol Microbiol* 61:394–406.
11. Singh D, et al. (2009) Regulation of ribonuclease E activity by the L4 ribosomal protein of Escherichia coli. *Proc Natl Acad Sci USA* 106:864–869.
12. Sawers G (1999) The aerobic/anaerobic interface. *Curr Opin Microbiol* 2:181–187.
13. Unden G, Bongaerts J (1997) Alternative respiratory pathways of Escherichia coli: Energetics and transcriptional regulation in response to electron acceptors. *Biochim Biophys Acta* 1320:217–234.
14. Górna MW, Carpousis AJ, Luisi BF (2012) From conformational chaos to robust regulation: The structure and function of the multi-enzyme RNA degradosome. *Q Rev Biophys* 45:105–145.
15. Nurmohamed S, McKay AR, Robinson CV, Luisi BF (2010) Molecular recognition between Escherichia coli enolase and ribonuclease E. *Acta Crystallogr D Biol Crystallogr* 66:1036–1040.
16. Rico AI, Krupka M, Vicente M (2013) In the beginning, Escherichia coli assembled the proto-ring: An initial phase of division. *J Biol Chem* 288:20830–20836.
17. Faubladier M, Bouché JP (1994) Division inhibition gene dicF of Escherichia coli reveals a widespread group of prophage sequences in bacterial genomes. *J Bacteriol* 176: 1150–1156.
18. Faubladier M, Cam K, Bouché JP (1990) Escherichia coli cell division inhibitor DicF-RNA of the dicB operon. Evidence for its generation in vivo by transcription termination and by RNase III and RNase E-dependent processing. *J Mol Biol* 212:461–471.
19. Balasubramanian D, Ragunathan PT, Fei J, Vanderpool CK (2016) A prophage-encoded small RNA controls metabolism and cell division in *Escherichia coli*. *mSystems* 1:e00021-15.
20. Jin Y, Watt RM, Danchin A, Huang JD (2009) Small noncoding RNA GcvB is a novel regulator of acid resistance in Escherichia coli. *BMC Genomics* 10:165.
21. Tétart F, Bouché JP (1992) Regulation of the expression of the cell-cycle gene ftsZ by DicF antisense RNA. Division does not require a fixed number of FtsZ molecules. *Mol Microbiol* 6:615–620.
22. Aiba H (2007) Mechanism of RNA silencing by Hfq-binding small RNAs. *Curr Opin Microbiol* 10:134–139.
23. Vogel J, Luisi BF (2011) Hfq and its constellation of RNA. *Nat Rev Microbiol* 9:578–589.
24. Moll I, Afonyushkin T, Vytvytska O, Kaberdin VR, Bläsi U (2003) Coincident Hfq binding and RNase E cleavage sites on mRNA and small regulatory RNAs. *RNA* 9:1308–1314.
25. Møller T, et al. (2002) Hfq: A bacterial Sm-like protein that mediates RNA-RNA interaction. *Mol Cell* 9:23–30.
26. Sahagan BG, Dahlberg JE (1979) A small, unstable RNA molecule of Escherichia coli: Spot 42 RNA. I. Nucleotide sequence analysis. *J Mol Biol* 131:573–592.
27. Zhang A, et al. (2003) Global analysis of small RNA and mRNA targets of Hfq. *Mol Microbiol* 50:1111–1124.
28. Goldblum K, Apririon D (1981) Inactivation of the ribonucleic acid-processing enzyme ribonuclease E blocks cell division. *J Bacteriol* 146:128–132.
29. Drepper T, et al. (2007) Reporter proteins for in vivo fluorescence without oxygen. *Nat Biotechnol* 25:443–445.
30. Tamura M, et al. (2006) RNase E maintenance of proper FtsZ/FtsA ratio required for nonfilamentous growth of Escherichia coli cells but not for colony-forming ability. *J Bacteriol* 188:5145–5152.
31. Khemici V, Poljak L, Luisi BF, Carpousis AJ (2008) The RNase E of Escherichia coli is a membrane-binding protein. *Mol Microbiol* 70:799–813.
32. Izumi A, Otto B, Heddle J, Park SY, Tame JRH (2004) 2P005 crystal structure of heme binding protein P46 from *Bacteroides fragilis*. *Seibutsu Butsuri* 44:S111.
33. Dewilde S, Van Hauwaert ML, Peeters K, Vanfleteren J, Moens L (1999) Daphnia pulex didomain hemoglobin: Structure and evolution of polymeric hemoglobins and their coding genes. *Mol Biol Evol* 16:1208–1218.
34. Milani M, et al. (2005) Structural bases for heme binding and diatomic ligand recognition in truncated hemoglobins. *J Inorg Biochem* 99:97–109.
35. Morita T, Kawamoto H, Mizota T, Inada T, Aiba H (2004) Enolase in the RNA degradosome plays a crucial role in the rapid decay of glucose transporter mRNA in the response to phosphosugar stress in Escherichia coli. *Mol Microbiol* 54:1063–1075.
36. Díaz-Ramos A, Roig-Borrellas A, García-Melero A, López-Alemany R (2012) α-Enolase, a multifunctional protein: Its role on pathophysiological situations. *J Biomed Biotechnol* 2012:156795.
37. Kim JW, Dang CV (2005) Multifaceted roles of glycolytic enzymes. *Trends Biochem Sci* 30:142–150.
38. Campanella ME, Chu H, Low PS (2005) Assembly and regulation of a glycolytic enzyme complex on the human erythrocyte membrane. *Proc Natl Acad Sci USA* 102: 2402–2407.
39. Lopez-Barneo J, Pardal R, Ortega-Sáenz P (2001) Cellular mechanism of oxygen sensing. *Annu Rev Physiol* 63:259–287.
40. Schulz EC, Tietzel M, Tovy A, Ankri S, Ficner R (2011) Structure analysis of Entamoeba histolytica enolase. *Acta Crystallogr D Biol Crystallogr* 67:619–627.
41. Taylor EL, Taylor TN, Krings M (2009) Precambrian life. *Paleobotany: The Biology and Evolution of Fossil Plants*, ed Thomas NT (Academic, San Diego), pp 43–70.
42. Lyons TW, Reinhard CT, Planavsky NJ (2014) The rise of oxygen in Earth's early ocean and atmosphere. *Nature* 506:307–315.
43. Justice SS, Hunstad DA, Cegelski L, Hultgren SJ (2008) Morphological plasticity as a bacterial survival strategy. *Nat Rev Microbiol* 6:162–168.
44. Chauhan A, et al. (2006) Mycobacterium tuberculosis cells growing in macrophages are filamentous and deficient in FtsZ rings. *J Bacteriol* 188:1856–1865.
45. Piao Z, Sze CC, Barysheva O, Iida K, Yoshida S (2006) Temperature-regulated formation of mycelial mat-like biofilms by Legionella pneumophila. *Appl Environ Microbiol* 72:1613–1622.
46. Stackhouse RR, Faith NG, Kaspar CW, Czuprynski CJ, Wong AC (2012) Survival and virulence of Salmonella enterica serovar enteritidis filaments induced by reduced water activity. *Appl Environ Microbiol* 78:2213–2220.
47. Yang J, Jain C, Schesser K (2008) RNase E regulates the Yersinia type 3 secretion system. *J Bacteriol* 190:3774–3778.
48. Erce MA, Low JK, Wilkins MR (2010) Analysis of the RNA degradosome complex in Vibrio angustum S14. *FEBS J* 277:5161–5173.
49. Aït-Bara S, Carpousis AJ (2015) RNA degradosomes in bacteria and chloroplasts: Classification, distribution and evolution of RNase E homologs. *Mol Microbiol* 97: 1021–1135.
50. Sambrook J, Fritsch EF, Maniatis T (1989) *Molecular Cloning: A Laboratory Manual* (Cold Spring Harbor Lab Press, Cold Spring Harbor, NY), 2nd Ed.
51. Omilusik K (2001) The role of metabolic by-product secretion by *Escherichia coli* in relation to intracellular NADH concentration and re-dox potential. *J Exp Microbiol Immunol* 1:1–8.
52. Covert MW, Knight EM, Reed JL, Herrgard MJ, Palsson BO (2004) Integrating high-throughput and computational data elucidates bacterial networks. *Nature* 429:92–96.
53. Wlaschin AP, Trinh CT, Carlson R, Srienc F (2006) The fractional contributions of elementary modes to the metabolism of Escherichia coli and their estimation from reaction entropies. *Metab Eng* 8:338–352.
54. Hemsley A, Arnheim N, Toney MD, Cortopassi G, Galas DJ (1989) A simple method for site-directed mutagenesis using the polymerase chain reaction. *Nucleic Acids Res* 17: 6545–6551.
55. Datsenko KA, Wanner BL (2000) One-step inactivation of chromosomal genes in Escherichia coli K-12 using PCR products. *Proc Natl Acad Sci USA* 97:6640–6645.
56. Arai R, Ueda H, Kitayama A, Kamiya N, Nagamune T (2001) Design of the linkers which effectively separate domains of a bifunctional fusion protein. *Protein Eng* 14: 529–532.
57. Towbin H, Staehelin T, Gordon J (1979) Electrophoretic transfer of proteins from polyacrylamide gels to nitrocellulose sheets: Procedure and some applications. *Proc Natl Acad Sci USA* 76:4350–4354.
58. Laemmli UK (1970) Cleavage of structural proteins during the assembly of the head of bacteriophage T4. *Nature* 227:680–685.
59. Hale CA, de Boer PA (1999) Recruitment of ZipA to the septal ring of Escherichia coli is dependent on FtsZ and independent of FtsA. *J Bacteriol* 181:167–176.
60. Chen C, Deutscher MP (2010) RNase R is a highly unstable protein regulated by growth phase and stress. *RNA* 16:667–672.
61. Lin-Chao S, Cohen SN (1991) The rate of processing and degradation of antisense RNAI regulates the replication of ColE1-type plasmids in vivo. *Cell* 65:1233–1242.
62. Brandi G, Schiavano GF, Albano A, Cattabeni F, Cantoni O (1989) The effect of K2Cr2O7 on the growth and morphology of Escherichia coli. *Biol Trace Elem Res* 21: 271–275.
63. Scheu PD, Steinmetz PA, Dempwolff F, Graumann PL, Unden G (2014) Polar localization of a tripartite complex of the two-component system DcuS/DcuR and the transporter DctA in Escherichia coli depends on the sensor kinase DcuS. *PLoS One* 9:e115534.
64. Hammarlöf DL, Liljas L, Hughes D (2011) Temperature-sensitive mutants of RNase E in Salmonella enterica. *J Bacteriol* 193:6639–6650.
65. Dagert M, Ehrlich SD (1979) Prolonged incubation in calcium chloride improves the competence of Escherichia coli cells. *Gene* 6:23–28.
66. Blattner FR, et al. (1997) The complete genome sequence of Escherichia coli K-12. *Science* 277:1453–1462.
67. Reister M, et al. (2014) Complete genome sequence of the gram-negative probiotic Escherichia coli strain Nissle 1917. *J Biotechnol* 187:106–107.